# Ground and excited state prototropic reactions in 2-(2′-methoxyphenyl)-3*H*-imidazo[4,5-*b*]pyridine †

**Somes K. Das and Sneh K. Dogra ***

*Department of Chemistry, Indian Institute of Technology, Kanpur, Kanpur-208016, India*

***Received (in Cambridge) 8th April 1998, Accepted 22nd September 1998***

The absorption, fluorescence and fluorescence excitation spectra of 2-(2′-methoxyphenyl)-3*H*-imidazo[4,5-*b*]-pyridine (2-MPIP) have been studied in five different solvents and at different acid–base concentrations. Semi-empirical quantum mechanical calculations have been carried out to supplement the experimental results. Spectral characteristics of 2-MPIP in different solvents and semi-empirical quantum mechanical calculations suggest the presence of both a-1 and b-1 isomers. The observation of a single exponential decay and one lifetime suggests an equilibrium between the isomers. Out of five monocations two kinds of monocations (MC's) are possible, one from protonation of $N^1$ (MC1) and the second from protonation of $N^4$ (MC2) atoms. Spectral characteristics and semi-empirical calculations carried out on MC's neglect the presence of isomer b-1. Only one kind of dication and one kind of monoanion are formed by protonating both the nitrogen atoms ($N^1$ and $N^4$) and deprotonating the >NH atom respectively. p$K_a$ and p$K_a$* values for the various prototropic reactions are determined and discussed.

## 1. Introduction

The photophysical and photochemical processes of benzimidazoles [BI's] are very well studied, because of their importance in chemistry, industry and biology.[1,2] It is well established that the site of protonation in benzimidazole[3–7] is at $N^3$. The absorption

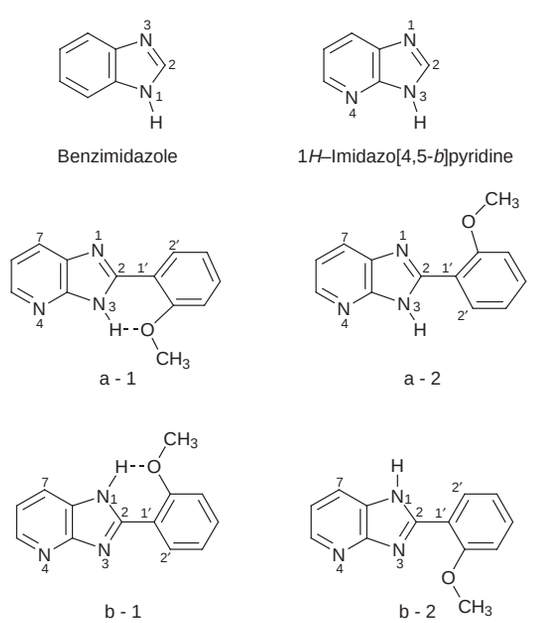


spectra of the benzimidazoles are hardly affected on protonation, whereas the fluorescence spectra of the monocation (MC) of BI's depend upon the nature of the substituents on the BI moiety. In case I, the fluorescence spectra of the MC's are either similar to the absorption spectra, slightly blue shifted or remain unchanged. This is assigned to the π–π* transition. In case II, the fluorescence spectra of the MC's are very red shifted in comparison to those of the neutral BI and this is due to the charge transfer transition. In case III, dual fluorescence is observed, possessing the characteristics of molecules belonging to case I and case II. It is observed that the presence of an electron donating group on the benzene ring and the electron withdrawing group on the imidazole moiety[5,6] induces the charge transfer character in the fluorescence emission.

On the other hand, the introduction of an additional heteroatom (N) with similar basicity to that of the imidazole nitrogen in the 2-substituent of BI (*e.g.*, 2-(2′-pyridyl)benzimidazole, 2-PyBI;[8] 2-(4′-pyridyl)benzimidazole, 4-PyBI;[9] 2-(3′-hydroxy-2′-pyridyl)benzimidazole, 2-HPyBI[10]) imparts complicated but interesting behaviour as the heteroatom in the pyridine ring may compete with the imidazole nitrogen in their affinity towards the proton in the ground or the excited states. We have been actively involved in studying the photophysics of the heterocyclic molecules in different environments.[11–14] With the aim of furthering our knowledge, we have synthesized a 2-substituted imidazo[4,5-*b*]pyridine having the same number of =N– atoms as 2-PyBI [two basic nitrogen atoms (–N=), one in the imidazole ($N^1$) and the other in the benzene ring ($N^4$) condensed to the imidazole moiety]. Since our main interest is to study the acid–base properties in the $S_1$ state, we have studied the molecule as 2-(2′-methoxyphenyl)-3*H*-imidazo[4,5-*b*]-pyridine (2-MPIP). The reason being that in general the presence of a phenyl group at the 2-position of heterocyclic molecules, like benzazoles,[7] increases the fluorescence quantum yield. Thus this study presents the effects of the solvents and the acid–base concentrations on the spectral characteristics of 2-MPIP. We have also tried to compare the experimental results with those obtained from semi-empirical quantum mechanical calculations, carried out on the neutral and the monocationic species.

## 2. Materials and methods

2-MPIP was synthesized by refluxing equivalent amounts of 2,3-diaminopyridine and *o*-methoxybenzoic acid in polyphosphoric acid at 160 °C as described in the literature.[15] 2-MPIP was purified by repeated crystallization from methanol. AnalR grade cyclohexane (S. D. Fine Chemicals), commercial ethanol, acetonitrile, methanol and dioxane (all E. Merck ) were further purified as described in the literature.[16] Triply distilled water was used for the preparation of aqueous solutions.

† Supplementary data are available (SUPPL. NO. 57444 pp. 2) from the British Library. For details of the Supplementary Publications Scheme, see 'Instructions for Authors' *J. Chem. Soc.*, *Perkin Trans. 2*, available *via* the RSC Web page (http://www.rsc.org/authors).

**Table 1** Absorption band maxima ($\lambda_{max}^{ab}$), log $\varepsilon_{max}$, fluorescence band maxima ($\lambda_{max}^{fl}$), and fluorescence quantum yield ($\varphi_{fl}$) of 2-MPIP in different solvents

| Solvents | $\lambda_{max}^{ab}$/nm (log $\varepsilon_{max}$) | | | $\lambda_{max}^{fl}$/nm ($\varphi_{fl}$) | | | |
|---|---|---|---|---|---|---|---|
| Dioxane | 333 | 318 | 298 | 337 | *352* | 369 | 389 |
| | (3.95) | (4.07) | (3.80) | | (0.36) | | |
| Acetonitrile | 332 | 319 | 297 | 335 | *352* | 368 | 386 |
| | (4.0) | (4.08) | (3.78) | | (0.43) | | |
| Ethanol | 331 | 320 | 297 | 338 | *353* | 369 | — |
| | (3.95) | (4.07) | (3.84) | | (0.41) | | |
| Methanol | 331 | 320 | 298 | 340 | *354* | 372 | — |
| | (3.95) | (4.07) | (3.84) | | (0.51) | | |
| Water | 332 | 320 | 298 | 342 | *361* | — | — |
| (pH = 6.8) | (3.86) | (3.99) | (3.83) | | (0.56) | | |
| Water | 338 | 304 | — | *400*[a] | *430*[b] | — | — |
| (pH = 2.0) | (3.96) | (3.72) | | (0.18) | (0.20) | | |
| Water | 364 | 319 | — | | *476* | — | — |
| ($H_o$ = −4) | (3.83) | (3.95) | | | (0.04) | | |
| Water | 340 | 315 | — | 346 | *361* | 377 | — |
| (pH = 14) | (3.48) | (3.85) | | | (0.29) | | |

[a] $\lambda_{exc}$ = 328 nm. [b] $\lambda_{exc}$ = 358 nm.

The procedure used for the preparation of solutions, adjustment of the pH in the range 3–11, as well as higher acid and base concentrations was the same as described in our recent papers.[17,18] The details of the instruments used to record absorption, fluorescence and fluorescence excitation spectra, to measure the excited state lifetimes and pH are the same as described earlier.[17,18] The fluorescence and fluorescence excitation spectra depicted in the figures are corrected ones. The fluorescence quantum yields ($\varphi_{fl}$) have been calculated from solutions having absorbance less than 0.1, using quinine sulfate in 2 M $H_2SO_4$ as a reference[19] ($\varphi_{fl}$ = 0.55). The concentration of the fluorophore was $1 \times 10^{-5}$ to $1 \times 10^{-4}$ M when prototropic reactions were studied.

## 3. Results and discussion

### 3.1 Solvent effects

The absorption and the fluorescence spectra of 2-MPIP have been recorded in five solvents. The spectral characteristics of 2-MPIP could not be studied in cyclohexane because of its insolubility. The relevant data are given in Table 1. Graphical presentations of the spectra are available as supplementary data. As for other benzimidazole derivatives,[5,6,8] the absorption spectrum of 2-MPIP is insensitive to the polarity and hydrogen bond formation capacity of the solvents, except for a slight loss of vibrational structure in polar protic solvents.

Unlike the absorption spectrum, a small but definite red shift is observed in the fluorescence spectrum with an increase in the polarity of the solvents (*i.e.*, in going from dioxane to water). The fluorescence spectrum of 2-MPIP is structured in non-polar solvents and becomes diffuse in polar solvents. The structure of the spectrum can be explained by a vibrational frequency of 1330 ± 60 $cm^{-1}$, which is similar to the frequencies observed in 2-phenyl substituted derivatives of benzimidazoles.[20–23] The fluorescence quantum yield increases with an increase in the polarity and protic nature of the solvents. The fluorescence spectrum has also been studied by excitation at different wavelengths towards the red side of the band maximum to see the red edge effect.[24] No change is observed either in the band maximum or in the fluorescence quantum yield. As it is well known that the solvent relaxation times of these solvents are only a few picoseconds, thus the fluorescence will occur from the most relaxed excited state.[25,26]

The fluorescence excitation spectra recorded at different emission wavelengths in different solvents resemble each other and also the absorption spectrum of 2-MPIP. This indicates that the geometry of the molecule does not change

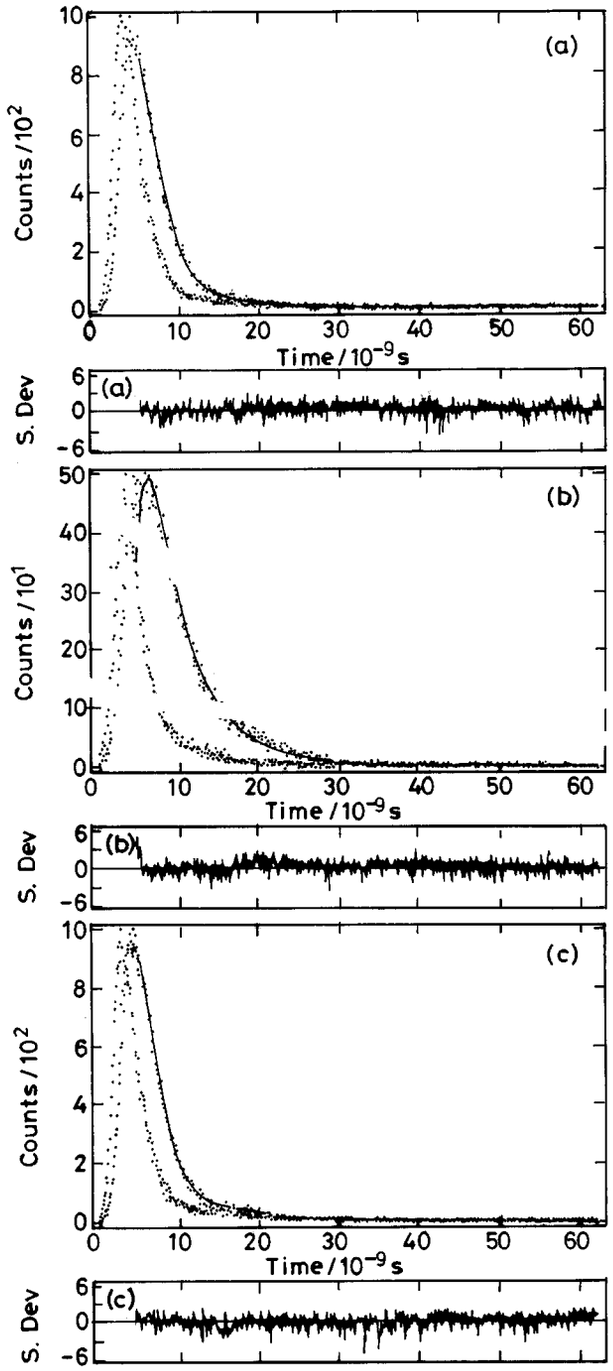


**Fig. 1** Fluorescence decay curves of 2-MPIP in water at different pH and different emission wavelengths ($\lambda_{em}$). $\lambda_{exc}$ = 337 nm. (a) pH = 6.8, $\lambda_{em}$ = 362 nm; (b) pH = 2.0, $\lambda_{em}$ = 410 nm; (c) pH = 2.0, $\lambda_{em}$ = 490 nm.

on excitation to the $S_1$ state. This is substantiated by the mirror image relationship observed between the absorption and the fluorescence spectra of the molecule, as well as the very small Stokes shifts observed for 2-MPIP in different solvents (356 $cm^{-1}$ in dioxane and 880 $cm^{-1}$ in water).

The excited state lifetimes were measured in four solvents by exciting at 337 nm, and the decay curve for 2-MPIP in water at pH 6.8 is shown in Fig. 1a. The fluorescence intensity in each case followed a single exponential decay having $\chi^2$ as 1.17. The data are given in Table 2. The radiative ($k_r$) and the non-radiative ($k_{nr}$) decay rate constants were calculated from the $\varphi_{fl}$ and the lifetime ($\tau$) using eqns. (1) and (2).[27]

$$k_r = \varphi_{fl}/\tau \quad (1)$$

$$k_{nr} = 1/\tau - k_r \quad (2)$$

The values of $k_r$ and $k_{nr}$, along with the fluorescence quantum yields are given in Table 2. It is evident from the results that the values of $k_r$ do not change, but those of $k_{nr}$ decrease with an increase in the polarity of the solvents. The increase in the fluorescence quantum yield of 2-MPIP is due to the decrease in the rate of the non-radiative processes.

Two isomers of 2-MPIP and two rotamers of each isomer were considered: a-1, a-2, b-1 and b-2. The PCMODEL program[28] was used to find the starting geometry of each molecule. This program enabled us to draw the structure, optimize roughly the geometry using the MM2 force field and generate the corresponding coordinates. The ground state geometries of all the species were then fully optimized using the AM1 method[29] (QCMP 137, MOPAC 6/PC). The ground state dipole moment ($\mu_g$), heat of formation, the total energy, ionization potential, dihedral angle and the charge density at each basic centre are given in Table 3. The transition energy $\Delta E_{i-j}$, corresponding to the excitation of an electron from the orbital $\varphi_i$ (occupied in the ground state) to $\varphi_j$ (unoccupied in the excited state) has been calculated using CNDO/S-CI calculations.[30] The transition energies for the first two transitions, along with the dipole moments in these states are given in Table 3. The charge densities in the first excited singlet state at all the basic centres have also been obtained by the CNDO/S-CI[31] method and are given in Table 3.

Three different kinds of isomers are possible for imidazo[4,5-*b*]pyridine: a, b and c. Comparison of the NH–CH coupling constants of imidazo[4,5-*b*]pyridine with the coupling constants[32] of the three fixed methyl derivatives eliminates the possibility of isomer c. Although the NMR studies cannot distinguish between isomer a and b, comparison of the dipole moments measured in benzene (1.99 D) with those calculated by the AM1 method suggests that isomer a will be the main component in benzene.[33] Based on the values of the heats of formation and the total energy in the gas phase (non-polar solvents) isomer b is less stable than isomer a by 14.9 kJ mol$^{-1}$. This could be due to the repulsive interactions between the lone pairs of $N^3$ and $N^4$. Similar behaviour is also observed in 2-(3′-hydroxy-2′-pyridyl)benzimidazole.[10] However, in polar/protic solvents (say for example water), isomer b becomes more stable when dipolar interactions are taken into account. These have been calculated using eqn. (3),[34,35] where f ($\varepsilon$) = ($\varepsilon - 1$)/($2\varepsilon + 1$), $d$ is the Onsager's cavity radius and $\varepsilon$ is the relative permittivity of the medium. Thus, it may be assumed that both the isomers (a and b) are present in the given solvent. A change in solvent polarity may change the proportions of the isomers with respect to each other. Examples are available where both kinds of structures for imidazo[4,5-*b*]pyridine are assumed in different substituted derivatives.[36,37]

$$\Delta E(\text{solv}) = -\mu_g^2/d^3 f(\varepsilon) \quad (3)$$

Considering the same arguments and using the same notations as used for imidazo[4,5-*b*]pyridine, the results given in Table 3 for the four species of 2-MPIP (a-1, a-2, b-1 and b-2) can be explained in the same manner, that is, among the four species, a-2 and b-2 are always unstable with respect to a-1 and b-1 even when dipolar solvation energies are added. Thus the presence of a-2 and b-2 can be neglected. Based on the following observations, it may be proposed that in any given solvent, there is an equilibrium between a-1 and b-1; (i) the presence of a very small Stokes shift and the mirror image relation observed between the absorption and the fluorescence spectra, (ii) the same fluorescence excitation spectra are observed at different emission wavelengths and also their

**Table 2** The excited state lifetimes ($\tau$), fluorescence quantum yields ($\varphi_{fl}$), rate constants for radiative ($k_r$) and non-radiative ($k_{nr}$) processes in different solvents

| Solvents | $\tau$/ns | $\varphi_{fl}$ | $k_r/10^{-8}$ s$^{-1}$ | $k_{nr}/10^{-8}$ s$^{-1}$ |
|---|---|---|---|---|
| Dioxane | 1.04 | 0.36 | 3.5 | 6.1 |
| Acetonitrile | 1.26 | 0.43 | 3.4 | 4.5 |
| Methanol | 1.46 | 0.51 | 3.5 | 3.3 |
| Water (pH = 6.8) | 1.63 | 0.56 | 3.4 | 2.7 |
| Water (pH = 2) | 1.82,[a] 1.37[b] | — | — | — |

[a] $\lambda_{em}$ = 410 nm. [b] $\lambda_{em}$ = 490 nm.

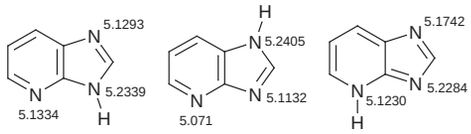


a b c

| | a | b | c |
|---|---|---|---|
| $\Delta H_f$/kJ mol$^{-1}$ | 327.7 | 342.4 | 389.2 |
| *E*/eV | -1456.164 | -1456.010 | -1455.525 |
| *E*/eV (solvated in water) | -1456.192 | -1456.494 | -1456.101 |
| $\mu_g$/D | 1.30 | 5.28 | 5.28 |
| IP/eV | 9.263 | 9.274 | 9.133 |

**Table 3** Calculated characteristics of the rotamers/isomers of 2-MPIP in the ground and excited states

| Characteristics | | | Rotamers/Isomers a-1 | a-2 | b-1 | b-2 |
|---|---|---|---|---|---|---|
| $\Delta H_f^o$/kJ mol$^{-1}$ | | | 278.2 | 291.1 | 291.7 | 305.2 |
| $E$ ($S_o$)/eV | | | −2754.875 | −2754.711 | −2754.735 | −2754.596 |
| $E$ ($S_o$)/eV (in water) | | | −2755.032 | −2754.828 | −2755.327 | −2754.945 |
| IP/eV | | | 8.685 | 8.862 | 8.743 | 8.992 |
| $\mu_g$/D | | | 3.21 | 2.79 | 6.11 | 5.55 |
| Dihedral angle ($N^{1\,a}$–$C^2$–$C^{1'}$–$C^{2'}$)/° | | | 145.4 | −63.4 | 146.8 | 86.4 |
| $r$($C^2$–$C^{1'}$)/A° | | | 1.465 | 1.466 | 1.466 | 1.468 |
| Transition energies/nm | $S_o$–$S_1$ | | 321.3 | 302.2 | 323.7 | 298.0 |
| | $S_o$–$S_2$ | | 285.0 | 275.6 | 280.1 | 275.0 |
| $\mu_e$/D | $S_1$ | | 5.90 | 5.71 | 7.05 | 8.02 |
| | $S_2$ | | 2.20 | 1.99 | 2.50 | 3.10 |
| Charge densities | $S_o$ | $N^1$ | 5.136 | 5.110 | 5.209 | 5.224 |
| | | $N^3$ | 5.203 | 5.225 | 5.121 | 5.096 |
| | | $N^4$ | 5.132 | 5.135 | 5.076 | 5.072 |
| | $S_1$ | $N^1$ | 5.323 | 5.293 | 5.211 | 5.197 |
| | | $N^3$ | 5.211 | 5.199 | 5.333 | 5.312 |
| | | $N^4$ | 5.318 | 5.325 | 5.311 | 5.341 |

[a] $N^3$ for a isomer.

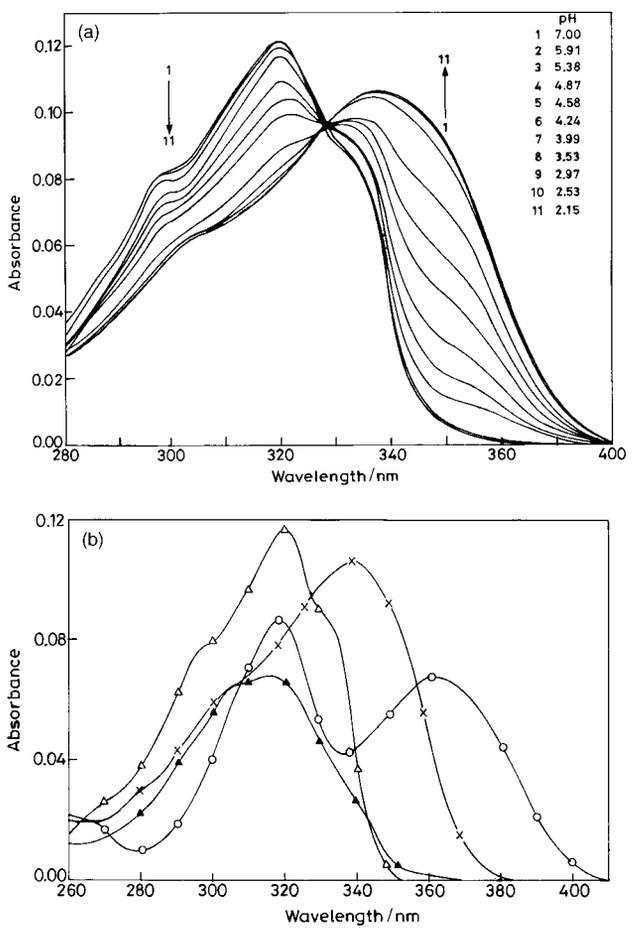


**Fig. 2** (a) Changes in absorption spectra of 2-MPIP in water with variation of acid concentration in the pH range 7–2. [2-MPIP] = $1 \times 10^{-5}$ M. (b) Absorption spectra of different prototropic species of 2-MPIP. [2-MPIP] = $1 \times 10^{-5}$ M. Δ—Δ—Δ, Neutral (pH = 6.8); x—x—x, Monocation (pH = 2.0); ○—○—○, Dication ($H_o = -4.0$); ▲—▲—▲, Monoanion (pH = 14.0).

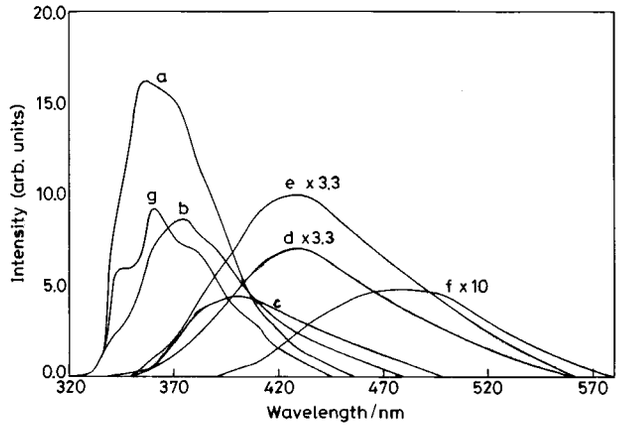


**Fig. 3** Fluorescence spectra of 2-MPIP in different acid–base concentrations and $\lambda_{exc}$. [2-MPIP] = $1 \times 10^{-5}$ M. a, pH = 6.8, $\lambda_{exc}$ = 328 nm; b, pH = 4.2, $\lambda_{exc}$ = 328; c, pH = 2.0, $\lambda_{exc}$ = 328; d, pH = 4.2, $\lambda_{exc}$ = 358; e, pH = 2.0, $\lambda_{exc}$ = 358; f, $H_o = -4.0$, $\lambda_{exc}$ = 358; g, pH = 14.0, $\lambda_{exc}$ = 320.

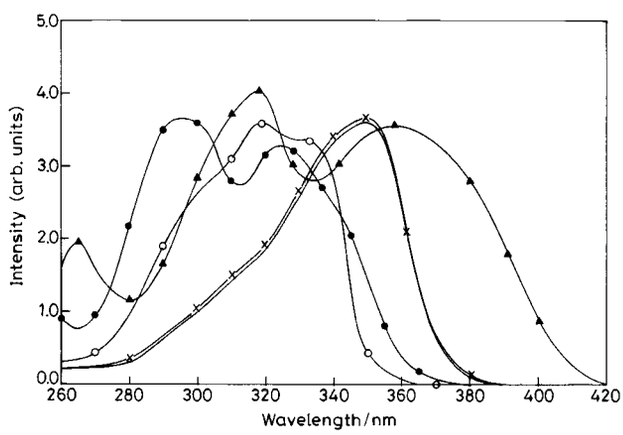


**Fig. 4** Fluorescence excitation spectra of the various species of 2-MPIP in water. [2-MPIP] = $1 \times 10^{-5}$ M. ——, $\lambda_{em}$ = 510 nm, pH = 4.2; ○—○—○, $\lambda_{em}$ = 370 nm, pH = 4.2; ●—●—●, $\lambda_{em}$ = 370 nm, pH = 2.0; x—x—x, $\lambda_{em}$ = 510 nm, pH = 2.0; ▲—▲—▲, $\lambda_{em}$ = 510 nm, $H_o = -4.0$.

resemblance to the absorption spectrum, (iii) similar transitions predicted by CNDO/S-CI for a-1 and b-1 and, (iv) the fluorescence decay follows a single exponential. The instability of the rotamers a-2 and b-2 could be due to the repulsion between the lone pairs of the methoxy oxygen and the =N– atom. Similar behaviour is also observed in 2-(2′-methoxyphenyl)benzimidazole,[22] 2-(2′-methoxyphenyl)naphth[2,3-*d*]-imidazole,[38] 2-(2′-3-hydroxypyridyl)benzimidazole[10] and 2-(2′-pyridyl)benzimidazole.[8]

All the transitions predicted by the CNDO/S-CI method for the rotamers a-1 and b-1 are π–π* in nature. This is supported by the large values found for the molar extinction coefficients and the fluorescence quantum yields. The agreement between the experimental and theoretical values is quite good in the long wavelength band of 2-MPIP, considering the approximations used in the calculations. As observed in the case of 2-phenyl substituted derivatives of benzimidazole,[20] the similarity of absorption band maxima and the vibrational frequency observed in the fluorescence spectrum of 2-MPIP, led us to predict that the long wavelength transition in 2-MPIP is also localized on the phenyl ring and is perturbed by the imidazo[4,5-*b*]pyridine ring.

It is well known that the flexibility of the molecules in the excited states[39] increases the non-radiative decay rate constants of these states and decreases the fluorescence quantum yield. The increase in the fluorescence quantum yields, decrease in the non-radiative decay rate constants and the vibrational structure observed in the fluorescence spectra suggest that the 2-MPIP molecule is more planar in the $S_1$ state than in the $S_o$ state. This indicates that the charge flow takes place from the phenyl ring to the imidazo[4,5-*b*]pyridine in the $S_1$ state. This is substantiated by the red shift observed in the fluorescence band maxima with an increase in polarity and hydrogen bond formation capacity of the solvents and the increase in the dipole moment upon excitation to the $S_1$ state (see Table 3).

### 3.2 Effect of pH

Fig. 2a depicts the absorption spectrum of 2-MPIP in the pH range of 2–7. It is clear from Fig. 2a that a shoulder develops in the absorption spectrum of 2-MPIP at ~350 nm with a decrease in pH, followed by a red shifted band maximum at 338 nm without a shoulder at pH 2.0 with only one isosbestic point at 328 nm in the pH range 2–7. A further red shift in the absorption spectrum of the monocation (MC) of 2-MPIP is observed with an increase in acid strength (Fig. 2b). A blue shifted 315 nm absorption band maximum with a shoulder at 340 nm was observed at pH >14 (Fig. 2b).

The fluorescence spectra of the ionic species present in the pH range 2–7 depend upon the excitation wavelength ($\lambda_{exc}$). For example, at $\lambda_{exc}$ 328 nm (the isosbestic point) and pH 2, the fluorescence band maximum is observed at 400 nm, whereas it shifts to 430 nm when $\lambda_{exc} \geq 340$ nm. On the other hand, at pH 4.2, the fluorescence band maximum observed in the former case is at 375 nm, whereas in the latter case it is at 430 nm (Fig. 3). The band widths at half the maximum height (BWHMH) observed at 400 and 430 nm are 4808 and 4592 $cm^{-1}$ respectively. Fluorescence excitation spectra recorded at 370 nm and at 510 nm are different from each other (Fig. 4),

as well as from the absorption spectrum recorded at pH 2.0. The fluorescence decays of the species at pH 2 were recorded at $\lambda_{em} = 410$ nm and 490 nm (Figs. 1b and 1c). The fluorescence decay in each case followed a single exponential with good $\chi^2$ values and residual plots. The values of the lifetimes observed at 410 and 490 nm are 1.82 ns ($\tau_{410}$) and 1.37 ns ($\tau_{490}$) respectively. The spectral characteristics of 2-MPIP in different non-aqueous solvents were also studied at different acid concentrations and the relevant data are compiled in Table 4. The short wavelength (SW) fluorescence band maximum is nearly insensitive to polarity, whereas that of the long wavelength (LW) emission shifts to the red as the polarity of the solvent increases.

Only one large red shifted (476 nm) fluorescence band is observed at $H_o$ −4, possessing similar fluorescence excitation spectra when recorded in the range of 440–510 nm, resembling the absorption spectra (Fig. 4) and having similar fluorescence band maxima and BWHMH when excited at a different wavelength. The fluorescence spectrum observed at pH 14, although possessing nearly the same fluorescence band maximum as the neutral (N) species, is better structured than the neutral species in an aqueous medium. The vibrational frequency observed in the fluorescence spectrum at pH 14 (1190 ± 60 $cm^{-1}$) is different from that of the neutral species (1330 ± 60 $cm^{-1}$). Similar behaviour is also observed in 2-phenylbenzimidazole.[20]

As mentioned earlier, there are two isomers (a-1 and b-1) for the neutral species of 2-MPIP. Three kinds of monocations (MC's, Fig. 5) can be obtained for each isomer. MC1 for a-1 and b-1 are resonance forms. Thus semi-empirical quantum mechanical calculations were performed on five species. The relevant data are given in Table 5. Under isolated conditions (non-polar solvents), MC1 (a-1) is the most stable, whereas MC3 (a-1) is the least stable. Taking into account the dipolar interactions, MC2 (a-1) is the most stable in the aqueous medium and MC1 (a-1) is the least. This is because of the large dipole moment of the MC2 (a-1) in comparison to MC1 (a-1).

It is well established that if π–π* is the lowest energy transition, the absorption and fluorescence spectra of the neutral species are red shifted on protonation of the =N– atom.[40] Furthermore, the p$K_a$ values for the protonation of =N– in pyridine and benzimidazole vary between 4.0 to 6.0. Thus the red shifts observed in the absorption and the fluorescence spectra of the neutral 2-MPIP in the pH range 2–7 are due to the formation of MC's, protonating either of the =N– atoms in any of the isomers. On the other hand, a further red shift observed at $H_o$ −4 is due to the formation of the dication (DC), protonating both the =N– atoms. A further red shift observed in the absorption spectrum and the different vibrational structure seen in the emission spectrum of 2-MPIP at pH 14 are due to the deprotonation of the >NH moiety and the formation of the monoanion (MA).

Fig. 2a shows a fairly good isosbestic point in the absorption spectrum of 2-MPIP on decreasing pH. The non-perfect crossing of all the curves is consistent with the presence of two

**Table 4** The absorption and the fluorescence band maxima of 2-MPIP in different solvents under acidic conditions ($H_2SO_4$)

| Solvents | [Acid]/M | $\lambda_{max}^{ab}$/nm | $\lambda_{max}^{fl}$/nm | |
|---|---|---|---|---|
| | | | $\lambda_{exc}^{a}$ = 328 nm | $\lambda_{exc}^{b}$ = 358 nm |
| Water | $10^{-2}$ | *338* | 400 | 430 |
| Ethanol | 0.2 | 352 (sh), *337* | 412 | 415 |
| Acetonitrile | 0.005 | *347*, 304 (sh) | 410 | 420 |
| Dioxane | 0.0074 | *345*, 310 (sh) | 407 | 414 |

[a] $\lambda_{exc}$ = 300, 315 nm. [b] $\lambda_{exc}$ = 345, 375 nm.

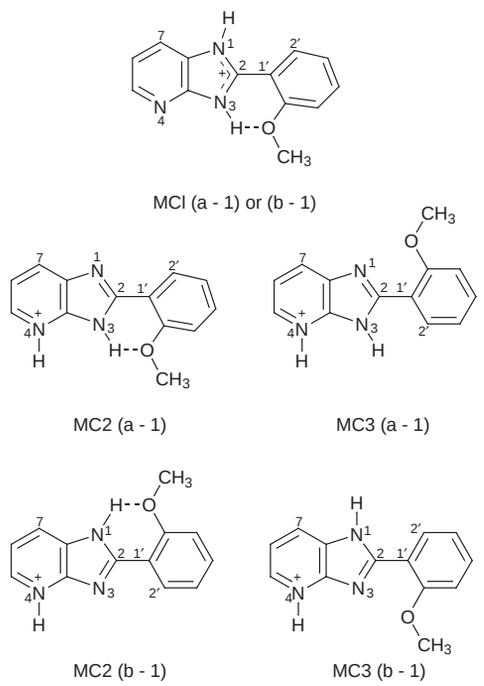


**Fig. 5** Structures of different probable monocations of 2-MPIP.

**Table 5** Calculated characteristics of the different monocations of 2-MPIP

| Characteristics | | | MC1 (a-1) or (b-1) | MC2 (a-1) | MC3 (a-1) | MC2 (b-1) | MC3 (b-1) |
|---|---|---|---|---|---|---|---|
| $\Delta H$/kJ $mol^{-1}$ | | | 850.7 | 885.6 | 902.0 | 865.0 | 881.9 |
| GS Energy/eV | | | −2762.597 | −2762.236 | −2762.066 | −2762.450 | −2762.274 |
| GS Energy/eV (solvated in water) | | | −2762.690 | −2763.583 | −2763.198 | −2762.832 | −2763.271 |
| IP/eV | | | 12.712 | 12.071 | 11.924 | 12.143 | 11.998 |
| $\mu_g$/D | | | 2.40 | 9.09 | 9.94 | 7.24 | 7.98 |
| Dihedral angle ($N^{1\,a}$–$C^2$–$C^{1'}$–$C^{2'}$)/° | | | 149.2 | 149.9 | −58.9 | 155.9 | 50.27 |
| $r$($C^2$–$C^{1'}$)/A° | | | 1.4545 | 1.4587 | 1.4570 | 1.4570 | 1.4586 |
| Transition energies/nm | $S_o$–$S_1$ | | 360 | 351 | 340 | 360 | 345 |
| | $S_o$–$S_2$ | | 310 | 307 | 299 | 305 | 301 |
| | $S_o$–$S_3$ | | 272 | 290 | 282 | 264 | 275 |
| Charge densities | $S_o$ | $N^1$ | 5.169 | 5.107 | 5.070 | 5.191 | 5.210 |
| | | $N^3$ | 5.143 | 5.212 | 5.230 | 5.167 | 5.126 |
| | | $N^4$ | 5.082 | 5.096 | 5.100 | 5.079 | 5.071 |
| | $S_1$ | $N^1$ | 5.202 | 5.218 | 5.268 | 5.172 | 5.201 |
| | | $N^3$ | 5.194 | 5.173 | 5.181 | 5.263 | 2.266 |
| | | $N^4$ | 5.267 | 5.237 | 5.240 | 5.202 | 5.233 |
| $\mu_e$/D | $S_1$ | | 9.97 | 9.56 | 13.11 | 5.88 | 12.15 |
| | $S_2$ | | 7.83 | 2.20 | 8.87 | 7.83 | 3.71 |

[a] $N^3$ for (a–1) isomers.

monocations with slightly different absorption spectra and slightly different p$K_a$s. A similar kind of explanation can also be given in the pH/$H_o$ range of 2 to −4 for the DC–MC equilibrium. Based on the two emission band maxima, two distinctly different fluorescence excitation spectra at each emission maximum and two lifetimes in the pH range 2–7 suggest the presence of two MC's, whereas one emission band maximum and similar fluorescence excitation spectra when recorded in the range of 440 to 510 nm, led us to conclude there is only one kind of DC.

As mentioned above, there are two basic centres in each isomer a-1 and b-1 and five different possible monocations can be formed (Fig. 5). MC3 (a-1) and MC3 (b-1) can be neglected on the basis that both are unstable with respect to MC1 (a-1) by 52 kJ mol$^{-1}$ and 31.2 kJ mol$^{-1}$ respectively under isolated conditions and by 37 kJ mol$^{-1}$ and 30.1 kJ mol$^{-1}$ when compared with MC2 (a-1) after taking into account the solvation energies in water. Thus the proportions of MC3 (a-1) and MC3 (b-1) at room temperature in the $S_o$ state will be negligible. The results given in Table 5 show that the dipole moment of MC2 (b-1) decreases on excitation to $S_1$ from 7.24 to 5.88 D. This will lead to a blue shift in the emission spectrum of the MC2 as the solvent polarity increases. The results of Table 4 clearly show that the SW emission band maxima are insensitive and the LW emission band maxima are red shifted in going from dioxane to water. These results suggest that MC2 (b-1) can also be neglected.

To establish the site of protonation in the MC, we have first tried to compare the charge densities at the different basic centres of 2-MPIP. The data in Table 3 show that the charge densities at the two basic centres ($N^1$ and $N^4$) of neutral 2-MPIP are similar, both in the ground and the first excited singlet states. Thus the charge density data cannot differentiate between the $N^1$ and $N^4$ sites. Although the use of an effective valence electron potential[41–43] as a reactivity index for the protonation of aza heterocyclic molecules in the $S_o$ and $S_1$ states is a good method, we have calculated the global minima at the basic centres using the potential energy mapping program. This method also considers the charge densities at a particular basic centre of interest plus the effective charges of the rest of the atoms in the molecule. The greater the depth of the potential well, the greater are the chances of protonation on the basic centre. Fig. 6 depicts the electrostatic potential energy map for 2-MPIP using the VSSPC computer program.[44] The results show that the site $N^1$ is more reactive (−112 kJ mol$^{-1}$) than the site $N^4$ (−95.2 kJ mol$^{-1}$), but the difference is not very large. Thus both the monocations can be present in the solution, which is established by the fluorescence excitation spectra recorded at 370 and 510 nm, and by the two fluorescence bands observed when excitation occurs at different wavelengths. The results of Tables 1, 4 and 5 and Fig. 1 suggest that both the MC's (MC1 and MC2 of a-1) are formed simultaneously, but their proportions are different in different solvents. Their relative proportions depend upon the solvent polarity. For example, MC1 (a-1), which is less polar than MC2 (a-1), will have a larger population in comparison to MC2 (a-1) in less polar solvents, whereas the reverse is true for MC2 (a-1) in polar solvents. This is substantiated by the absorption spectrum of 2-MPIP in different solvents under acidic conditions, *i.e.*, there are two band systems in each solvent except water. The LW absorption band maxima shift to SW band maxima with an increase in the polarity of the solvents. Thus the LW absorption and fluorescence band maxima are assigned to MC1 (a-1) and the SW absorption and fluorescence band maxima to MC2 (a-1). This is substantiated by the fact that: (i) the fluorescence band maximum of MC1 (a-1) is sensitive to the environment (Table 4), whereas that of the MC2 (a-1) is not sensitive to the solvent polarity. This could be due to the large change in the dipole moment of MC1 (a-1), (from 2.40 to 9.97 D) on excitation to the $S_1$ state, whereas that of MC2 (a-1) changes from 9.1 to 9.6 D and (ii) the transition wavelengths determined for MC1 (a-1) and MC2 (a-1), using the CNDO/S-CI method agree well with the experimental results.

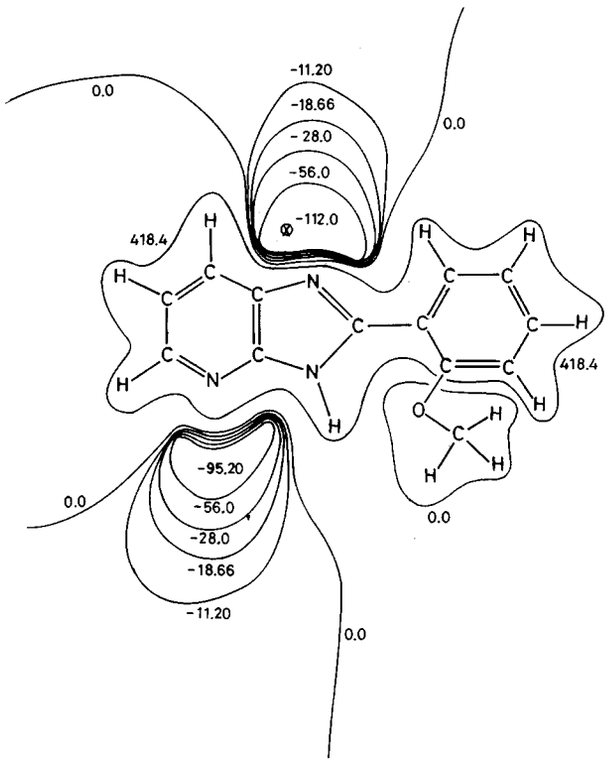


**Fig. 6** Electrostatic potential map for 2-MPIP in the ground state (values shown are in kJ mol$^{-1}$).

### 3.3 Acidity constants

The p$K_a$ values for the DC–MC, the MC–N and the N–MA equilibria have been determined from the absorption data using the Henderson–Hasselbach equation. The values of the slopes observed in each case (1.0 ± 0.1) clearly suggest the presence of equilibria between the conjugate acid–base pairs, *i.e.*, the dication–monocations and the monocations–neutral. The values so obtained are given above the arrows in Fig. 7. The agreement between the p$K_a$ value for the MC's–N equilibrium obtained by us and that observed by Elvidge *et al.*[45] substantiates our point. It may also be pointed out here that even if a small difference in the p$K_a$ values for the MC1–N and MC2–N equilibria is present, the continuous change in the absorption spectra (Fig. 2) did not allow us to calculate the p$K_a$ values for each MC–N equilibrium. Further similar behaviour has been observed in 2-(4′-aminophenyl)-benzoxazole,[12] 2-(4′-aminophenyl)benzothiazole[46] and 2-(4′-*N*,*N*-dimethylaminophenyl)benzothiazole.[13]

The excited state p$K_a$ (p$K_a$*) values for the DC–MC and the MC–N equilibria have been determined from the fluorimetric titrations and are given below the arrows in Fig. 7. The value for the MC–N equilibrium (4.3) resembles that of the ground state p$K_a$, indicating that the lifetimes of the conjugate acid–base species are too short for the establishment of an equilibrium in the $S_1$ state, whereas the value for the DC–MC equilibrium (0.5) suggests that =N– becomes a stronger base on excitation to the $S_1$ state. The p$K_a$* for the N–MA equilibrium could not be determined because of overlapping band maxima and fluorescence intensities of both the species.

## Conclusions

The present study has shown that 2-MPIP is more planar in the $S_1$ state in comparison to the $S_o$ state. This is supported by:

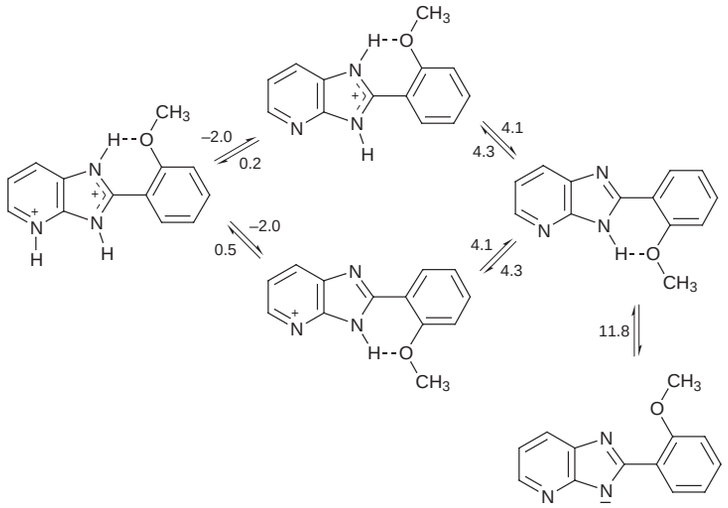


**Fig. 7** Schematic diagram for the different prototropic reactions of 2-MPIP. Values above and below the arrows indicate the p$K_a$ and p$K_a$* values respectively.

(i) the vibrational structure in the fluorescence spectra, and (ii) a decrease in the rate of the non-radiative processes. Absorption, fluorescence and fluorescence excitation spectra and time resolved studies have shown that the isomers a-1 and b-1 are present in equilibrium in different solvents, whereas the effect of acid concentrations on the spectral characteristics of 2-MPIP in different solvents combined with AM1 calculations rule out the presence of isomer b-1 for the MC's. The proportion of less polar MC1 (a-1) in comparison to more polar MC2 (a-1) is larger in less polar environments and the proportion of MC1 (a-1) decreases as the polarity or the ionic strength of the medium increases. This is supported by the higher $\mu_g$ of MC2 (a-1), fluorescence excitation and fluorescence spectra. Only one kind of DC and MA are formed. The MC–N equilibrium is not established in the $S_1$ state in aqueous media but whichever basic nitrogen is not protonated in the MC becomes a stronger base on excitation to the $S_1$ state.

## Acknowledgements

The authors thank the Department of Science and Technology, New Delhi for the financial support of Project No. SP/SI/H-39/96.

## References

1 P. N. Preston, in *Benzimidazoles and Cogeneric Tricyclic Compounds*, vol. 40, Part I, Wiley-Interscience, New York, 1981.
2 P. N. Preston, in *Benzimidazoles and Cogeneric Tricyclic Compounds*, vol. 40, Part II, Wiley-Interscience, New York, 1981.
3 M. Kondo and H. Kuwano, *Bull. Chem. Soc. Jpn.*, 1969, **42**, 1433.
4 P. C. Tway and L. J. C. Love, *J. Phys. Chem.*, 1982, **86**, 5223, 5227.
5 M. Krishnamurthy, P. Phaniraj and S. K. Dogra, *J. Chem. Soc., Perkin Trans. 2*, 1986, 1917.
6 H. K. Sinha and S. K. Dogra, *J. Chem. Soc., Perkin Trans. 2*, 1987, 1465.
7 S. K. Dogra, *Proc. Indian Acad. Sci.*, 1992, **104**, 635.
8 F. R. Prieto, M. Mosquera and M. Novo, *J. Phys. Chem.*, 1990, **94**, 8536 and references listed therein.
9 M. Novo, M. Mosquera and F. R. Prieto, *Can. J. Chem.*, 1992, **70**, 823.
10 M. Mosquera, M. C. R. Rodriguez and F. Rodriguez-Prieto, *J. Phys. Chem.*, *A*, 1997, **101**, 2266 and references listed therein.
11 M. Swaminathan and S. K. Dogra, *J. Am. Chem. Soc.*, 1983, **105**, 6223.
12 J. K. Dey and S. K. Dogra, *Chem. Phys.*, 1990, **149**, 97.
13 J. K. Dey and S. K. Dogra, *J. Phys. Chem.*, 1994, **98**, 3638.
14 S. Santra and S. K. Dogra, *Chem. Phys.*, 1996, **207**, 103.
15 R. W. Middleton and D. G. Wibberley, *J. Heterocycl. Chem.*, 1980, **17**, 1757.
16 J. A. Riddick and W. B. Bunger, in *Organic Solvents*, Wiley-Interscience, New York, 1970.
17 S. Santra and S. K. Dogra, *Chem. Phys.*, 1998, **226**, 229.
18 S. K. Das and S. K. Dogra, *J. Chem. Soc., Faraday Trans.*, 1998, **94**, 139.
19 G. G. Guilbault, in *Practical Fluorescence*, Dekker, New York, 1971, p. 13.
20 A. K. Mishra and S. K. Dogra, *Spectrochim. Acta*, *Part A*, 1983, **39**, 609.
21 A. K. Mishra and S. K. Dogra, *Bull. Chem. Soc. Jpn.*, 1985, **58**, 3587.
22 H. K. Sinha and S. K. Dogra, *Chem. Phys.*, 1986, **102**, 337.
23 H. K. Sinha and S. K. Dogra, *J. Photochem.*, 1987, **36**, 149.
24 A. P. Demchenko, in *Topics in Fluorescence Spectroscopy: Biochemical Applications*, vol. 3, ed. J. R. Lakowicz, Plenum Press, New York, 1993, p. 65.
25 N. Weichmann, H. Port, W. Frey, F. Larmer and T. Elsasser, *J. Phys. Chem.*, 1991, **95**, 1918.
26 E. W. Castner, Jr., B. Bagchi, M. Moroncelli, S. P. Webb, A. J. Ruggiero and G. R. Flemming, *Ber. Bunsen-Ges. Phys. Chem.*, 1988, **92**, 363.
27 N. J. Turro, in *Modern Molecular Photochemistry*, Benjamin Publishing Inc., London, 1978, p. 176.
28 J. Hinze and H. H. Jaffe, *J. Am. Chem. Soc.*, 1962, **84**, 540.
29 M. J. S. Dewar, E. G. Zeobish, E. F. Healy and J. J. P. Stewart, *J. Am. Chem. Soc.*, 1985, **107**, 3902.
30 J. DelBene and H. H. Jaffe, *J. Chem. Phys.*, 1962, **48**, 1807.
31 A. Kumar and P. C. Mishra, *QCPE Bull.*, 1989, **9**, 67.
32 J. Elguero, C. Marzin, A. R. Katritzky and P. Linda, in *Tautomerism in Heterocycles*, Academic Press, New York, 1976, p. 521.
33 Y. M. Yutilov, N. R. Kal'nitskii and R. M. Bystrova, *Khim. Geterotsikl. Soedin*, 1971, **10**, 1436.
34 N. Mataga and T. Kubata, in *Molecular Interactions and Electronic Spectra*, Marcel Dekker, New York, 1970.
35 J. F. Letard, R. Lapouyade and W. Retig, *Chem. Phys. Lett.*, 1994, **222**, 209.
36 E. Fasani, A. Albani, P. Savarino, G. Viscareli and E. Barni, *J. Heterocycl. Chem.*, 1993, **30**, 1041.
37 P. Savarino, G. Viscardi, R. Carpignano, A. Borda and E. Barni, *J. Heterocycl. Chem.*, 1989, **26**, 289.
38 S. K. Das and S. K. Dogra, unpublished results.
39 G. Kohler, *J. Photochem.*, 1987, **38**, 217.
40 J. F. Ireland and P. A. H. Wyatt, *Adv. Phys. Org. Chem.*, 1978, **12**, 131.
41 J. Spanget-Larsen, *J. Chem. Soc., Perkin Trans. 2*, 1985, 417.
42 J. Waluk, W. Rettig and J. Spangert-Larsen, *J. Phys. Chem.*, 1988, **92**, 6930.
43 J. Spanget-Larsen, *J. Phys. Org. Chem.*, 1995, **8**, 496 and references listed therein.
44 P. C. Mishra and B. P. Asthana, QCPE No. 039, *Quantum Chem. Program Exch. Bull.*, 1987, **9**, 176.
45 J. A. Elvidge, J. R. Jones, C. O. Brien, E. A. Evans and H. C. Sheppard, *J. Chem. Soc., Perkin Trans. 2*, 1973, 1889.
46 J. K. Dey and S. K. Dogra, *Bull. Chem. Soc. Jpn.*, 1991, **64**, 3142.

*Paper 8/02684J*